NAVAL POSTGRADUATE SCHOOL

MONTEREY, CALIFORNIA

THESIS

STUDY OF COMPOSITE JOINT STRENGTH WITH CARBON NANOTUBE REINFORCEMENT

by

Susan D. Faulkner

September 2008

Thesis Advisor:	Young W. Kwon
Second Reader:	Scott W. Bartlett

Approved for public release; distribution is unlimited.

THIS PAGE INTENTIONALLY LEFT BLANK

REPORT DOCUMENTATION PAGE			*Form Approved OMB No. 0704-0188*
Public reporting burden for this collection of information is estimated to average 1 hour per response, including the time for reviewing instruction, searching existing data sources, gathering and maintaining the data needed, and completing and reviewing the collection of information. Send comments regarding this burden estimate or any other aspect of this collection of information, including suggestions for reducing this burden, to Washington headquarters Services, Directorate for Information Operations and Reports, 1215 Jefferson Davis Highway, Suite 1204, Arlington, VA 22202-4302, and to the Office of Management and Budget, Paperwork Reduction Project (0704-0188) Washington DC 20503.			
1. AGENCY USE ONLY ***(Leave blank)***	**2. REPORT DATE** September 2008	**3. REPORT TYPE AND DATES COVERED** Master's Thesis	
4. TITLE AND SUBTITLE Study of Composite Joint Strength with Carbon Nanotube Reinforcement			**5. FUNDING NUMBERS**
6. AUTHOR(S) Susan D. Faulkner			
7. PERFORMING ORGANIZATION NAME(S) AND ADDRESS(ES) Naval Postgraduate School Monterey, CA 93943-5000			**8. PERFORMING ORGANIZATION REPORT NUMBER**
9. SPONSORING /MONITORING AGENCY NAME(S) AND ADDRESS(ES) N/A			**10. SPONSORING/MONITORING AGENCY REPORT NUMBER**
11. SUPPLEMENTARY NOTES The views expressed in this thesis are those of the author and do not reflect the official policy or position of the Department of Defense or the U.S. Government.			
12a. DISTRIBUTION / AVAILABILITY STATEMENT Approved for public release; distribution is unlimited.			**12b. DISTRIBUTION CODE**

13. ABSTRACT (maximum 200 words)

Strengthening of composite joints is a topic of recent research. The benefits of using locally applied carbon nanotubes to reinforce a carbon fiber composite joint were studied. The effect of carbon nanotubes on enhancing the fracture toughness and joint interface strength was investigated by performing Mode I, Mode II, and Mixed Mode I/Mode II fracture with and without carbon nanotubes applied locally at the joint interface. Furthermore, the effects of seawater absorption on Mode II fracture were investigated. Finally, an optimization of carbon nanotube concentration was performed. During the study, the image correlation technique was used to examine the fracture mechanisms altered by the introduction of carbon nanotubes. The experimental study showed that carbon nanotubes can increase the fracture toughness of the composite interface significantly, especially for Mode II, including a physical change in the fracture mechanism.

14. SUBJECT TERMS Carbon Nanotubes, CNT, Carbon Fiber Composite, Fracture Mechanics, Joint Strength Enhancement, Reinforcement, Mode I, Mode II, Mixed Mode I/Mode II			**15. NUMBER OF PAGES** 70
			16. PRICE CODE
17. SECURITY CLASSIFICATION OF REPORT Unclassified	**18. SECURITY CLASSIFICATION OF THIS PAGE** Unclassified	**19. SECURITY CLASSIFICATION OF ABSTRACT** Unclassified	**20. LIMITATION OF ABSTRACT** UU

NSN 7540-01-280-5500 Standard Form 298 (Rev. 2-89)
Prescribed by ANSI Std. 239-18

THIS PAGE INTENTIONALLY LEFT BLANK

Approved for public release; distribution is unlimited

STUDY OF COMPOSITE JOINT STRENGTH WITH CARBON NANOTUBE REINFORCEMENT

Susan D. Faulkner
Lieutenant, United States Navy
B.S., United States Naval Academy, 2000

Submitted in partial fulfillment of the
requirements for the degree of

MASTER OF SCIENCE IN MECHANICAL ENGINEERING

from the

NAVAL POSTGRADUATE SCHOOL
September 2008

Author: Susan D. Faulkner

Approved by: Prof. Young W. Kwon
Thesis Advisor

Scott W. Bartlett
Second Reader

Knox T. Millsaps
Chairman, Department of Mechanical and Astronautical Engineering

THIS PAGE INTENTIONALLY LEFT BLANK

ABSTRACT

Strengthening of composite joints is a topic of recent research. The benefits of using locally applied carbon nanotubes to reinforce a carbon fiber composite joint were studied. The effect of carbon nanotubes on enhancing the fracture toughness and joint interface strength was investigated by performing Mode I, Mode II, and Mixed Mode I/Mode II fracture with and without carbon nanotubes applied locally at the joint interface. Furthermore, the effects of seawater absorption on Mode II fracture were investigated. Finally, an optimization of carbon nanotube concentration was performed. During the study, the image correlation technique was used to examine the fracture mechanisms altered by the introduction of carbon nanotubes. The experimental study showed that carbon nanotubes can increase the fracture toughness of the composite interface significantly, especially for Mode II, including a physical change in the fracture mechanism.

THIS PAGE INTENTIONALLY LEFT BLANK

TABLE OF CONTENTS

LIST OF FIGURES

LIST OF TABLES

THIS PAGE INTENTIONALLY LEFT BLANK

ACKNOWLEDGMENTS

First and foremost, I would like to thank Dr. Young Kwon for his mentorship during the course of this research and throughout my graduate studies.

Thank you to Erik Rasmussen, Scott Bartlett, Doug Loup, and Tim Dapp from the Naval Surface Warfare Center Carderock Division (NSWCCD) team for "Advanced Hull Materials & Structures Technology (AHM&ST)" who provided crucial funding, materials, and technical guidance.

Chris Hicks from the Northrop Grumman Ship Systems Advanced Capabilities Group, Science and Technologies – Composites is also appreciated for providing technical guidance, specifically in the area of moisture effects testing.

THIS PAGE INTENTIONALLY LEFT BLANK

I. INTRODUCTION

A. BACKGROUND

In recent years, large composite structures have been incorporated into naval vessels to increase operational performance while lowering ownership costs [1]. The trend continues with new projects, such as the superstructure for DDG 1000. In particular, carbon fiber composite material provides high strength and stiffness while maintaining low weight. The joints of these large composite structures are the weakest point due to discontinuity of fiber reinforcement. The joints therefore have the largest failure rate [2]. Strengthening the composite joint will increase the strength of the entire composite structure. Research has shown that varying joint geometry can increase joint strength [3]. However, changing the joint geometry can depend on the loading condition. Ship structures undergo a variety of loading conditions, so varying the geometry is not always the ideal method of strengthening the joint. Another type of reinforcement is therefore required. Carbon nanotubes, with high strength and stiffness, provide a means to locally reinforce the joint while not sacrificing the integrity of the composite material.

Carbon nanotubes (CNT) are allotropes of carbon with a hexagonal lattice structure like graphite. The lattice structure forms a tube with nano-sized diameter. CNT can be several millimeters in length. They can be either single-walled or multi-walled, meaning an inner cylinder lies within the outer cylinder [4]. Although many strides have been made in the manufacture of CNT, they are still quite expensive. CNT have an extremely high elastic modulus (greater than 1 TPa) yet are lightweight [5]. Therefore, they are ideal for strengthening composite materials.

B. LITERATURE SURVEY

The elastic modulus of carbon nanotubes (CNT) is greater than one TPa, and CNT are 10 to 100 times stronger than the strongest steels [5]. The high strength and relatively low weight of CNT make them a prime candidate for composite material reinforcement. Much research has been performed documenting the ability of CNT to reinforce a variety of matrix materials such as various polymers and ceramics. One such study found high

interfacial shear stress and stronger interfacial adhesion between multi-walled CNT (MWNT) to epoxy than epoxy to epoxy. The same study found no increase in tensile strength due to MWNT reinforcement [6]. Another study explored the use of several different types of carbon nanotubes in a polymer composite. Young's modulus was doubled as a result of the reinforcement. The same study indicated that low diameter multi-walled carbon nanotubes were the ideal CNT for reinforcement due to their surface area characteristics [7].

Many studies have been conducted to determine the type of bonds formed between CNT and epoxy. The general conclusion is that CNT bond in three main ways: micromechanical interlocking, chemical bonding, and van der Waals bonding. While the CNT surface is quite smooth, it has been proposed that there are local non-uniformities in the CNT such as kinks, bends, and changes in diameter. It is at these local non-uniformities where micromechanical interlocking occurs [6]. Chemical bonding is possible, but it is not guaranteed [8]. Finally, van der Waals bonding certainly occurs, but a relatively weak bond forms. One study also proposes the effects of thermal properties. The coefficient of thermal expansion of CNT is much higher than that of the polymer matrix. As a result, residual compressive thermal stress is present after the polymer matrix hardens. This thermal stress results in closer contact between the CNT and polymer, which in turn increases micromechanical interlocking and non-bond interactions [6].

While the effects of uniform incorporation of carbon nanotubes within a polymer structure have been studied, only one study has documented the results of local reinforcement of a carbon fiber composite with CNT. The research focused on a composite scarf joint, which is applicable to the U.S. Navy. Several types of CNT were tried, including various multi-walled CNT as well as bamboo structured CNT. Additionally, two different CNT concentrations were used. The study found that under compression testing, the carbon fiber composite scarf joint was stronger when reinforced with CNT [9].

C. OBJECTIVES

The research presented in this paper builds on the aforementioned study. Widespread use of carbon nanotubes throughout a ship superstructure is too costly for the United States Navy. However, local reinforcement of the structure at its weakest points is possible. The fracture toughness of the locally reinforced joint must be studied to determine the impact of reinforcement. The purpose of this research is to determine the critical energy release rate, G, and crack propagation characteristics of CNT reinforced and non-reinforced carbon fiber/vinyl ester resin composite samples during Mode I, Mode II, and Mixed Mode I/Mode II fractures. Additionally, the effects of seawater absorption on Mode II critical energy release rate were studied. Finally, an optimization of CNT concentration was performed. A wide variety of samples were tested to show conclusively the impact of CNT reinforcement on fracture toughness. Sample sets varied in geometry and construction technique. The two construction techniques employed were hand lay-up and Vacuum Assisted Resin Transfer Molding (VARTM).

This research is in support of the Naval Surface Warfare Center Carderock Division (NSWCCD) team for "Advanced Hull Materials & Structures Technology (AHM&ST)." The seawater absorption testing was completed in support of Northrop Grumman Ship Systems Advanced Capabilities Group, Science and Technologies – Composites.

THIS PAGE INTENTIONALLY LEFT BLANK

II. COMPOSITE SAMPLE CONSTRUCTION

A. SAMPLE SPECIFICATION

Five sets of carbon fiber samples were constructed during the course of this research. Each set of samples consisted of resin only samples and CNT reinforced samples so results could be compared. Size and construction technique of the samples varied, which will be discussed later. However, the basic sample construction remained the same throughout the research. Samples consisted of carbon fiber composite specimens with a secondary bond at the interface layer and a pre-existing edge crack, as shown in Figure 1. The presence of the secondary bond is required to mimic joint construction. When constructing the scarf joint, one side is constructed and cured. The other side is then constructed directly on top of the existing side.

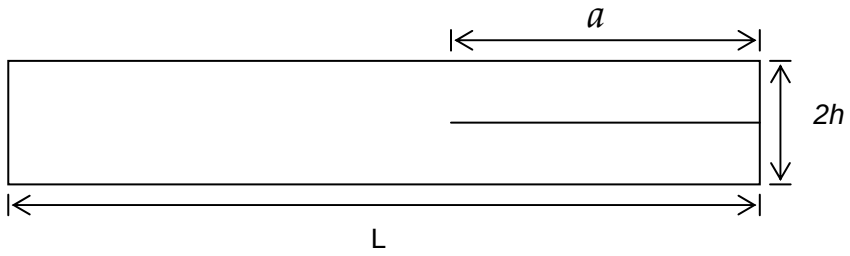

Figure 1. Sample geometry

where:

L = length
2h = thickness
a = initial crack length

1. Materials

A vinyl-ester matrix base, DERAKANE 510-A was used with TORAY T700CF carbon fiber weave. These materials were selected by the Naval Surface Warfare Center Carderock Division (NSWCCD) team for "Advanced Hull Materials & Structures Technology (AHM&ST)" since they are used for naval vessels. Hardening chemicals are

required to cure the resin. The hardening chemicals are Methyl Ethyl Ketone Peroxide (MEKP) and Cobalt Naphthenate (CoNap). These chemicals were used in concentrations recommended by the manufacturer of DERAKANE 510-A. A hardening time of 60 minutes was selected to allow ample time for sample construction. With ambient temperature between 70˚F and 80˚F, the combination of hardeners consisted of 1.25 %wt MEKP and 0.20 %wt CoNap to achieve the desired hardening time.

2. Construction Techniques

Two construction techniques were used during the research. First, a hand lay-up technique was employed. This is a relatively simplistic method of constructing carbon fiber composite specimens which involves minimal laboratory equipment. After proving the theory that fracture toughness is affected by CNT reinforcement, a more complex technique was employed. Vacuum Assisted Resin Transfer Molding (VARTM) is one of several construction techniques used in industry, thereby making it a logical choice of construction technique. While it involved more laboratory equipment and extensive trial and error to create suitable samples, it was imperative to prove local CNT reinforcement would be both useful and feasible by industry. Both the hand lay-up and VARTM techniques will be discussed in detail.

B. HAND LAY-UP TECHNIQUE

A detailed description of the hand layup procedure is provided in Table 1. In summary, a bottom carbon fiber plate was constructed first and cured. The bottom plate was then sanded and cleaned with acetone. Next, a wax paper insert of thickness 0.0038 cm (0.0015 in) was placed across the bottom plate for the initial crack. Next, acetone was used as a dispersing agent for CNT. This study used conventional multi-walled CNT with diameter 30nm+/-15nm and length 5-20μm. CNT surface concentration was 7.5 g/m^2. The selection of CNT as well as the selection of acetone as the dispersing agent was based on results from compression testing of CNT reinforced scarf joints [9]. After the acetone dried, the top plate was constructed on top of the bottom plate, forming a secondary bond between plates. After curing, samples were cut using the Jet Edge waterjet cutter.

Samples then underwent a post-cure treatment. Although the resin is mostly cured after 12 hours, it continues to cure over long periods of time. It is possible that material properties may change over time. Therefore, samples underwent a six-hour post-cure at 140°F to mimic long-term curing.

Table 1. Detailed hand lay-up sample construction procedure

Step 1	Attach a layer of porous non-permeable ply and peel ply to aluminum plate to serve as base for composite layup.	
Step 2	Cut carbon fiber fabric to desired size. Four layers of carbon fiber fabric were used to achieve desired thickness.	
Step 3	Manually apply resin compound to each sheet of carbon fiber fabric using a foam brush.	* See Figs. 2 and 3
Step 4	Immediately following completion of layup, wrap the composite in one layer of peel ply, one layer of porous non-permeable ply, and one layer of buffer ply.	
Step 5	Place composite plate in airtight vacuum bag. Apply vacuum. Vacuum removes trapped air in the composite structure and promotes absorption of excess resin by the buffer ply.	* See Fig. 4
Step 6	After 12-hour cure, remove the vacuum and composite plate. One-half of the sample has been constructed.	
Step 7	Sand the top of the composite plate with 100 grit sand paper to roughen the surface.	
Step 8	Clean with acetone and allow acetone to dry fully.	
Step 9	Attach delamination insert to desired area of composite plate.	* See Fig. 5
Step 10	Disperse CNT on top of composite plate and allow dispersing agent (acetone) to dry.	* See Fig. 6
Step 11	Construct top layer of sample by repeating steps 2-6.	* See Fig. 7
Step 12	Cut samples using Jet Edge waterjet cutter.	
Step 13	Post-cure samples at 140°F for six hours.	* Phases III-V only

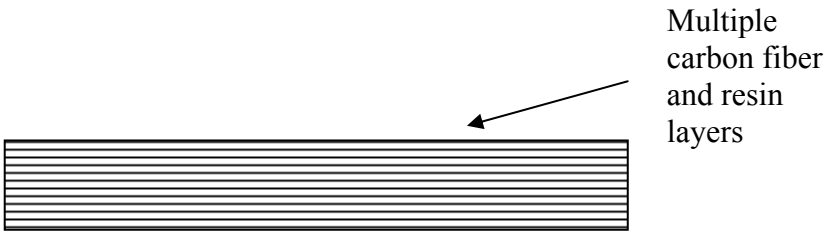

Figure 2. Side view of bottom plate

Figure 3. Image of composite sample prior to cure

Figure 4. Image of composite sample curing under vacuum

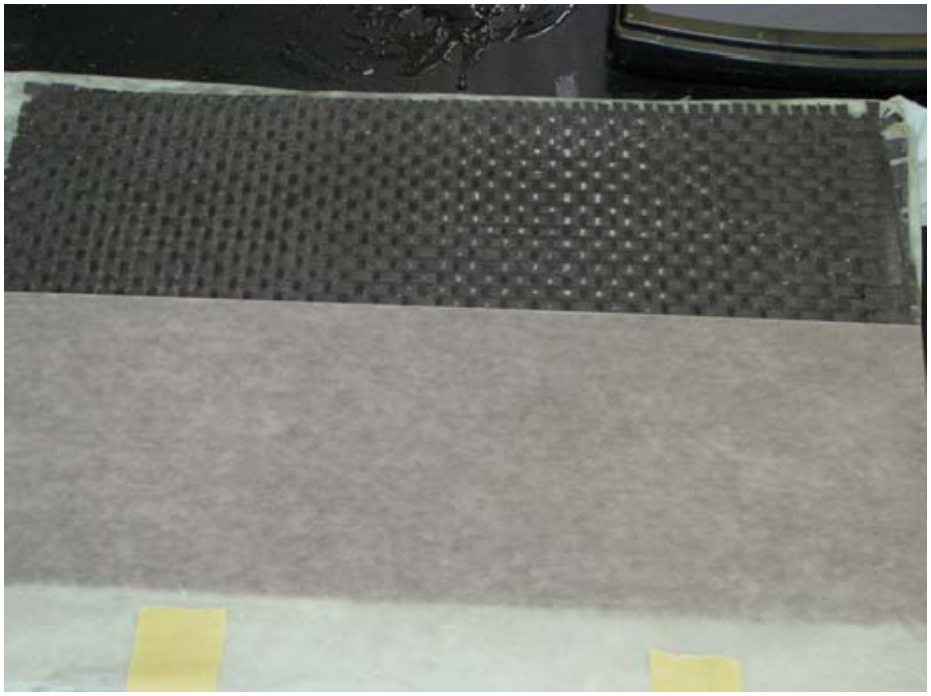

Figure 5. Image of cured bottom layer after surface preparation with delamination insert attached

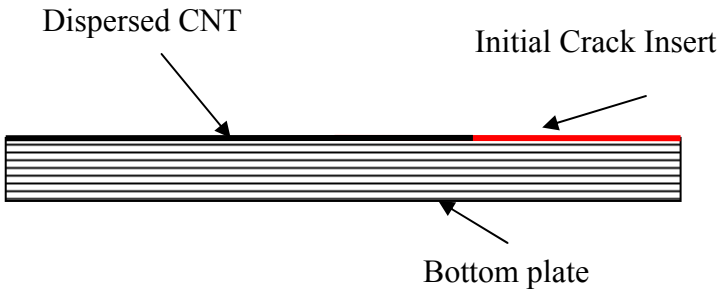

Figure 6. Side view of bottom plate with CNT

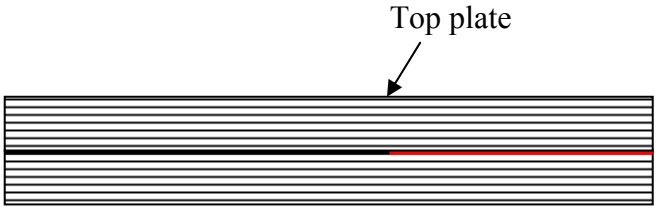

Figure 7. Side view of constructed sample

C. VACUUM ASSISTED RESIN TRANSFER MOLDING TECHNIQUE

A detailed description of the Vacuum Assisted Resin Transfer Molding (VARTM) procedure is provided in Table 2. In summary, the VARTM technique involves pulling resin through the layers of carbon fiber with a vacuum. Samples were constructed in the same manner as when using the hand lay-up technique, meaning a bottom carbon fiber plate was constructed first and cured. The bottom plate was then sanded and cleaned with acetone. When using the VARTM technique, Teflon film of thickness 0.0051 cm (0.002 in) was used as the delamination insert. Acetone was again used as the dispersing agent for applying CNT. CNT surface concentration was 7.5 g/m^2. After the acetone dried, layers of carbon fiber were stacked on the bottom plate and infused with resin. After curing, samples were cut using the Jet Edge waterjet cutter. Samples then underwent a post-cure treatment.

There was some concern that the CNT would be displaced when pulling the resin through the layers of carbon fiber. However, the CNT remained in place. This was a significant finding, since VARTM is a popular method for constructing carbon fiber composites in industry. No special technique will be needed when applying CNT locally. The CNT can simply be dispersed on the desired area and VARTM can be conducted.

Table 2. Detailed VARTM sample construction procedure

Step 1	Place a layer of peel ply on glass to serve as base for composite construction. Glass must be at least 1.27 cm (0.5 in) thick.	
Step 2	Cut carbon fiber fabric to desired size. Five layers of carbon fiber fabric were used to achieve desired thickness.	
Step 3	Stack carbon fiber fabric on top of peel ply.	* See Fig. 8
Step 4	Place a second layer of peel ply on top of carbon fiber fabric. Place a sheet of distribution media on top of peel ply.	
Step 5	Set up resin inlet and outlet tubing. Adequate tubing is required to ensure resin is not pulled into the vacuum source. A resin trap on the outlet side is recommended.	* See Figs. 9 and 10
Step 6	Attach plastic sheet using putty/tape. Plastic sheet will act as a vacuum bag.	
Step 7	Perform vacuum check and fix vacuum leaks. Vacuum of 26 inches Hg should be obtained. Continue applying vacuum.	
Step 8	Mix resin and hardeners. A cure time of 60 minutes was used for this research.	
Step 9	Wait approximately 10 minutes. Immediately after being mixed with hardeners, the resin produces air bubbles. Wait until air bubbles are no longer being produced.	* See Fig. 11
Step 10	Allow resin to flow into carbon fiber layers. Flow speed may be adjusted by adjusting vacuum. However, vacuum of 10 inches Hg should be maintained.	* See Figs. 12 and 13
Step 11	When carbon fiber layers are infused with resin and resin accumulates in the outlet tubing, clamp resin inlet to ensure air is not pulled into the sample. Infusion time depends on sample size and thickness. During this research, infusion time was roughly 5-10 minutes.	
Step 12	Maintain vacuum until resin hardens.	
Step 13	Allow sample to cure at least 12 hours before removing sample from VARTM set up. Construction of bottom plate is complete.	* See Fig. 2
Step 14	Sand the top of the composite plate with 100 grit sand paper to roughen the surface.	
Step 15	Clean with acetone and allow acetone to dry fully.	
Step 16	Attach delamination insert to desired area of composite plate.	* See Fig. 5
Step 17	Disperse CNT on top of composite plate and allow dispersing agent (acetone) to dry.	* See Fig. 6
Step 18	Construct top layer of sample by repeating steps 1-13.	* See Fig. 7
Step 19	Cut samples using Jet Edge waterjet cutter.	
Step 20	Post-cure samples at 140°F for six hours.	* Phases III-V only

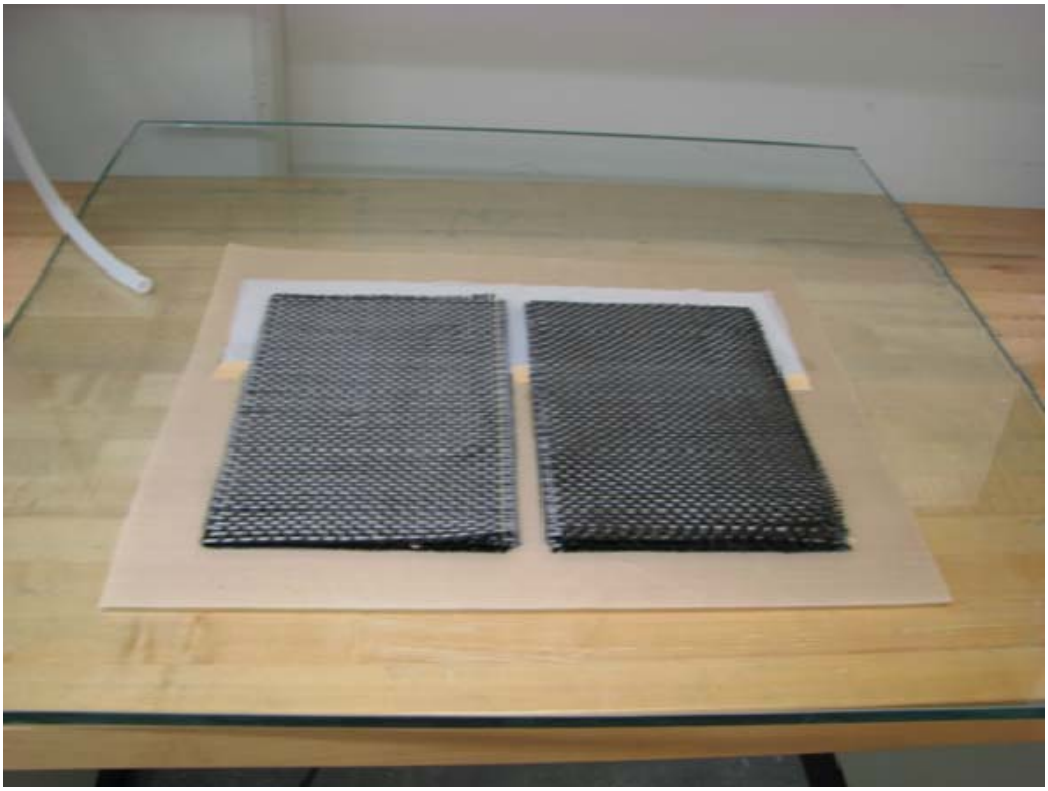

Figure 8. Layers of carbon fiber fabric stacked on peel ply

Figure 9. Inlet tubing set-up

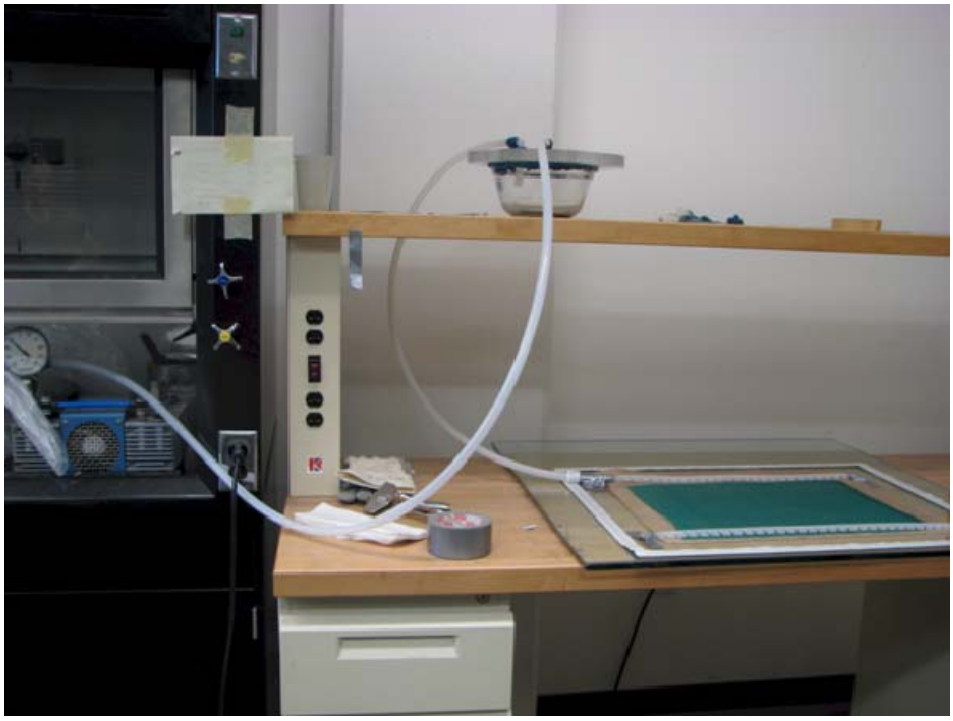

Figure 10. Outlet tubing set-up with resin trap

Figure 11. Vacuum applied during approximately 10- minute wait

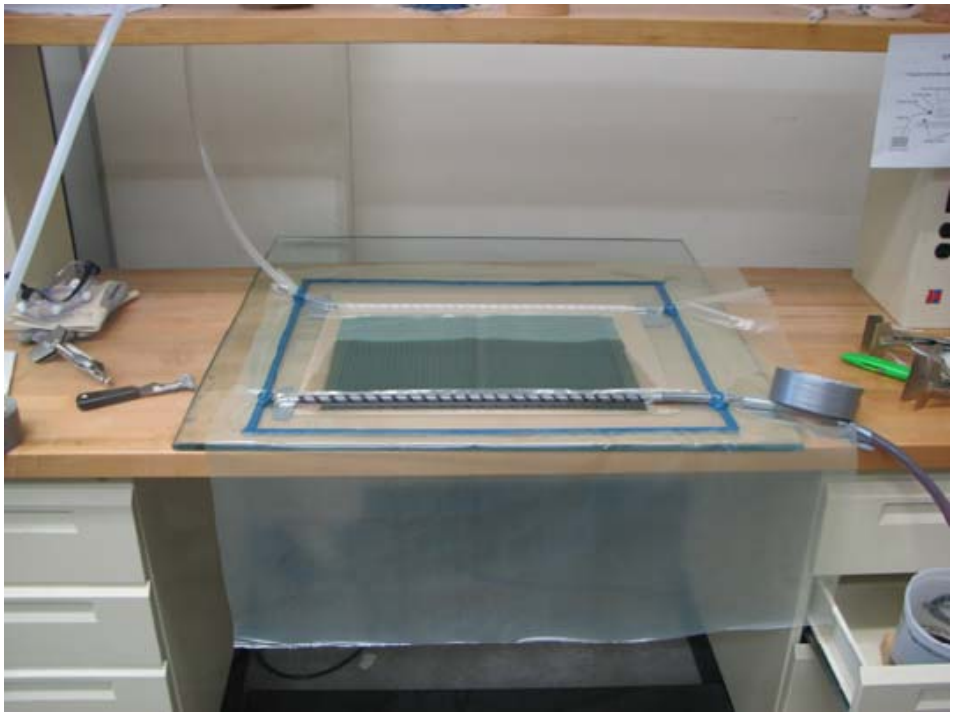

Figure 12. Resin flow through carbon fiber layers, showing inlet and outlet tubing

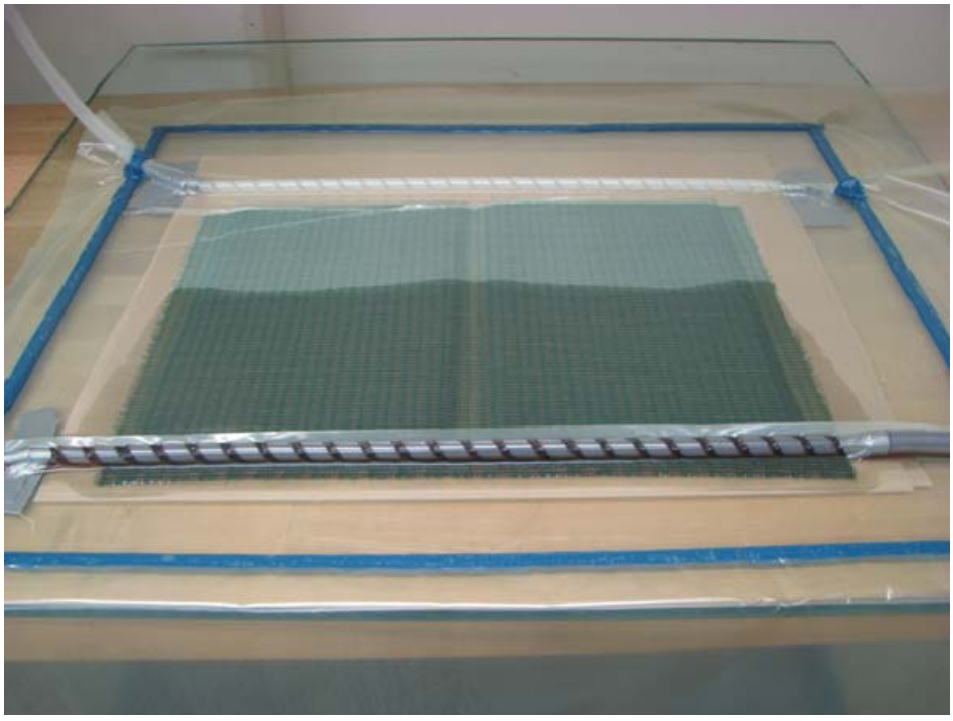

Figure 13. Resin flow through carbon fiber layers

THIS PAGE INTENTIONALLY LEFT BLANK

III. PHASES OF RESEARCH

A. PHASE I

Phase I was completed as a learning experience. Ten samples were constructed to practice the hand lay-up technique and dispersion of CNT. The samples were then tested to learn how to use the test equipment.

B. PHASE II

Phase II was completed to test the theory that fracture toughness is affected by CNT reinforcement. This phase consisted of large samples constructed via the hand lay-up technique. Samples were nominally 2.5 cm wide, 0.75 cm thick, and 40.5 cm in length. The large sample size was chosen so readily available laboratory equipment could be used during testing. The samples were tested in both Mode I and Mode II and critical energy release rate, G, was calculated.

C. PHASE III

After proving the theory, samples were constructed via the hand lay-up method and tested according to applicable ASTM standards. Sample size was reduced to a nominal 2.5 cm wide, 0.5 cm thick, and 14.0 cm in length. The purpose of this phase of research was to ensure sample size did not affect the impact of CNT reinforcement on fracture toughness. Additionally, a six-hour postcure at 140°F was conducted to mimic long term curing of the sample. The postcure was conducted on all subsequent phases. Testing was also expanded to include Mode I, Mode II, and Mixed Mode I/Mode II testing. Additionally, the effects of seawater absorption were studied during this phase of research.

D. PHASE IV

Once the theory was proven using the hand lay-up technique, samples were produced using the VARTM technique. The VARTM technique requires extensive laboratory supplies, and is one of the common techniques used in industry. The purpose of Phase IV was two-fold. First, a method of locally dispersing the CNT in the carbon

fiber composite was devised. Secondly, Mode II testing was repeated to ensure the effects of CNT reinforcement were not affected by the VARTM procedure. The effects of seawater absorption were also studied during this phase of research.

E. PHASE V

The final phase of research determined an optimum concentration of CNT. The effect of "banded CNT" was also studied. Previously, all CNT reinforced samples were constructed with CNT dispersed on the entire fracture surface. However, CNT reinforcement during this phase only extended 6 cm from the crack tip. "Banding" the CNT was done to determine the effect of localized reinforcement. Additionally, three concentrations of CNT were used: 5 g/m^2, 7.5 g/m^2, and 10 g/m^2. Samples were constructed via the VARTM technique. Mode II testing was completed.

IV. TESTING

A. OVERVIEW

Samples were tested using an Instron Tension/Compression Machine (Model Number: 4507/4500) with 10 kN load cell. Series IX computer software was used to control displacement and record displacement and load values. All tests were performed at the rate of 2.54 mm displacement per minute (0.1 in/min). Additionally, a Digital Image Correlation System was employed to record images during testing at the rate of 1 image per second. The Digital Image Correlation System was also used to measure strain fields around the crack during the crack initiation and growth.

B. MODE I

The applicable ASTM Standard was followed for Mode I testing. Mode I testing consisted of a double cantilever beam (DCB) test as shown in Figure 14 [10]. Piano hinges, used to apply the load, were attached to each sample using a commercially available 2-part epoxy. The following equation was used to determine critical energy release rate, G_I, through the Modified Beam Theory method [10]:

$$G_I = \frac{3P\delta}{2ba}$$

where:

P=load when crack propagates
δ =load point displacement
b=sample width
a=initial delamination length

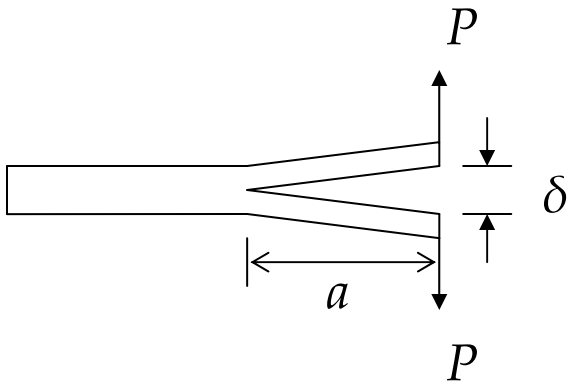

Figure 14. Double cantilever beam test for Mode I (i.e., crack opening) fracture

C. MODE II

No applicable ASTM Standard exists for pure Mode II fracture toughness testing. Mode II testing consisted of a three point bending test as shown in Figure 15. Because the crack lies in the midplane of the beam, only shear stress is applied to the crack. The following equation was used to determine Mode II critical energy release rate, G_{II} [11]:

$$G_{II} = \frac{3P_c^2}{64bE_{11}I}\left[a^2 + \frac{0.2h^2E_{11}}{G_{13}}\right]$$

where:

P_c=critical load when crack propagates
h=1/2 total thickness
b=sample width
a=initial crack length
$I = \frac{bh^3}{12}$

The selection of the critical load was based on both observation of crack propagation and a local maximum or slope change in the load versus displacement curve.

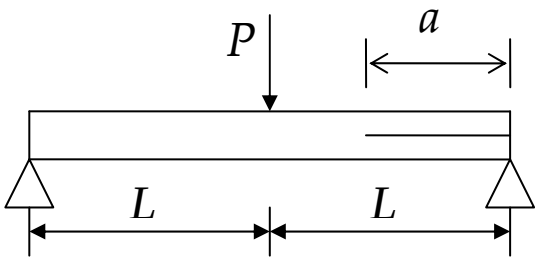

Figure 15. Three point bending test for Mode II (i.e., shearing mode)

Calculation of the Mode II critical energy release rate, G_{II}, was repeated using a compliance approach with the following equation [12]:

$$G_{II} = \frac{9a^2 P_c^2 C}{2b(2L^3 + 3a^3)}$$

where:

P_c=critical load when crack propagates
C=compliance
a=initial crack length
b=sample width
L=1/2 span length

It can be shown that the two methods are equivalent. The first method clearly delineates the contribution from transverse shear deformation. However, the first method requires material properties to be known as well as precise measurement of height and thickness of the sample. The second method, the compliance approach, does not require material properties to be known. Instead, the material properties are indirectly measured via the experimentally determined compliance. The contribution from transverse shear stress is also imbedded in the compliance measurement. Both equations were used to compute G_{II} for the present study.

D. MIXED MODE I/MODE II

The applicable ASTM Standard was used to guide Mixed Mode I/Mode II testing. Mixed Mode I/Mode II testing requires a special test rig as shown in Figure 16 [13].

Piano hinges, used to apply the load and secure the sample in the test rig, were attached to each sample using a commercially available 2-part epoxy. Multiple equations are necessary to calculate the Mixed Mode I/Mode II critical energy release rate. These equations can be found in the applicable ASTM Standard [13].

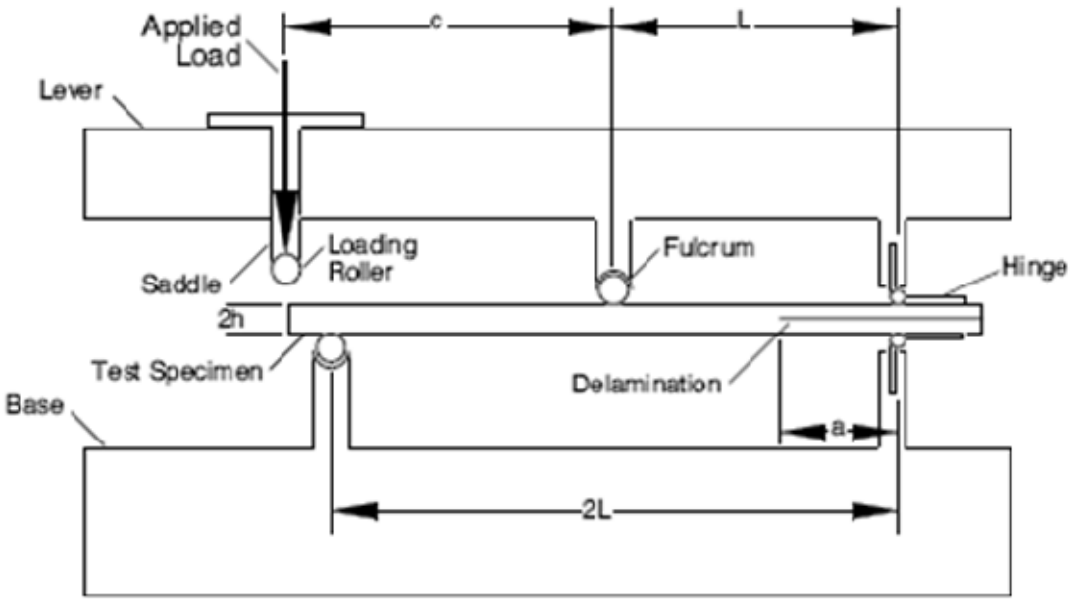

Figure 16. Mixed Mode I/Mode II test apparatus [From [13]]

E. SEAWATER ABSORPTION EFFECTS

To test the effects of seawater absorption on local CNT reinforcement, samples were soaked in seawater until saturation and then tested in Mode II. Seawater was mixed using substrate conforming to ASTM Standard D1141-98 and samples were soaked at room temperature, nominally 70-80 degrees Fahrenheit [14]. Dimensions and weight of each sample were recorded prior to soak. Seawater absorption was tracked by periodically weighing each sample during soaking. When weight no longer changed significantly, the samples were determined to be saturated and Mode II testing was conducted as described previously.

V. RESULTS AND DISCUSSION

A. MODE I

Mode I testing showed a small improvement in G_I when the interface joint was reinforced with CNT. Figure 17 displays the average values of normalized G_I for resin only samples and CNT samples from Phase III. Included in Appendix A are values of G_I for each sample. Standard deviation is also shown in the figure. Similar results were obtained for Phase II. Mode I crack propagation characteristics were also observed with no discernable difference between the CNT reinforced and non-reinforced samples. Since CNT reinforcement does not lead to a significant improvement of G_I, no further Mode I testing was completed.

The Digital Image Correlation System was used to plot normal strain perpendicular to crack orientation because the normal stress is the cause of crack opening. A representative image just prior to crack propagation is shown in Figure 18. CNT reinforced and non-reinforced images were very similar.

After testing, the samples were fully broken to inspect the cracked surface. Mode I samples revealed little difference between CNT reinforced and non-reinforced samples. Both CNT reinforced and non-reinforced samples had crack growth through the resin layers where the initial cracks were located.

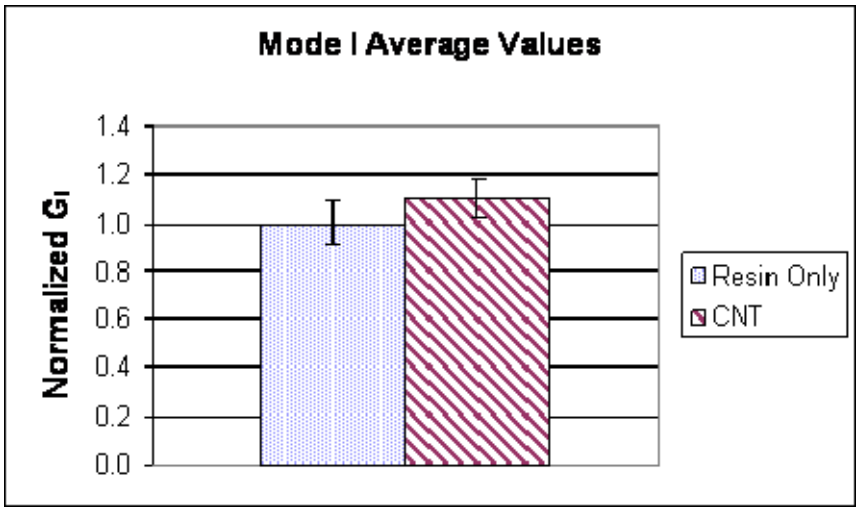

Figure 17. Mode I Normalized G_I Values

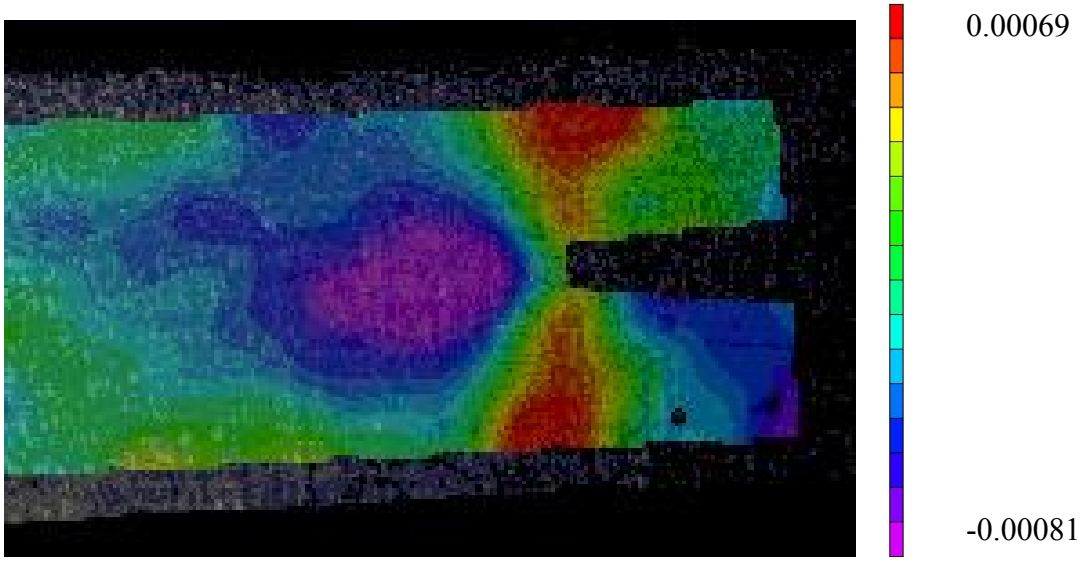

Figure 18. Image of transverse normal strain just prior to Mode I (opening mode) crack propagation

B. MODE II

Mode II testing resulted in a significant increase in G_{II} for the samples reinforced with CNT. Figure 19 displays the normalized average values of G_{II} for Phase III specimens. Again, standard deviation is also shown in the figure. As displayed by the standard deviation, the lowest CNT reinforced value is higher than the highest non-

reinforced value. Additionally, the average CNT reinforced G_{II} value was 27.6% higher than the average resin only G_{II} value. Appendix B includes G_{II} values for each sample.

The average value of G_{II} varied between the Phase II and Phase III. The average value of G_{II} for Phase II was 83% higher than that of Phase III. There are three potential causes for the discrepancy. First, Phase III samples underwent a post-cure treatment while Phase II samples did not. Over time, the material properties of carbon fiber composite may change due to continued curing of the resin. The post-cure treatment accelerates the long term curing. The second factor may be degradation of the uncatalyzed, uncured resin as a function of time. While CNT reinforced and non-reinforced samples in each phase were constructed at the same time, the two sample sets were fabricated several months apart. Finally, the specimen dimensions were different. Phase III sample size conformed to the ASTM Standard, while Phase II samples were larger. The ASTM standard is probably designed for aerospace laminates with thin layers and unidirectional fibers or tight fabric. The 9oz woven fabric from 12K rovings may be 'too coarse' for a smaller specimen size, resulting in a different value for Mode II critical energy release rate. Subsequent study should investigate the respective impact of post-cure treatment, resin degradation, and sample size.

Although the quantitative values of G_{II} were different from sample set to sample set, the effect of CNT reinforcement remained the same. The average CNT reinforced G_{II} value was 27.3% higher for Phase II and 27.6% higher for Phase III.

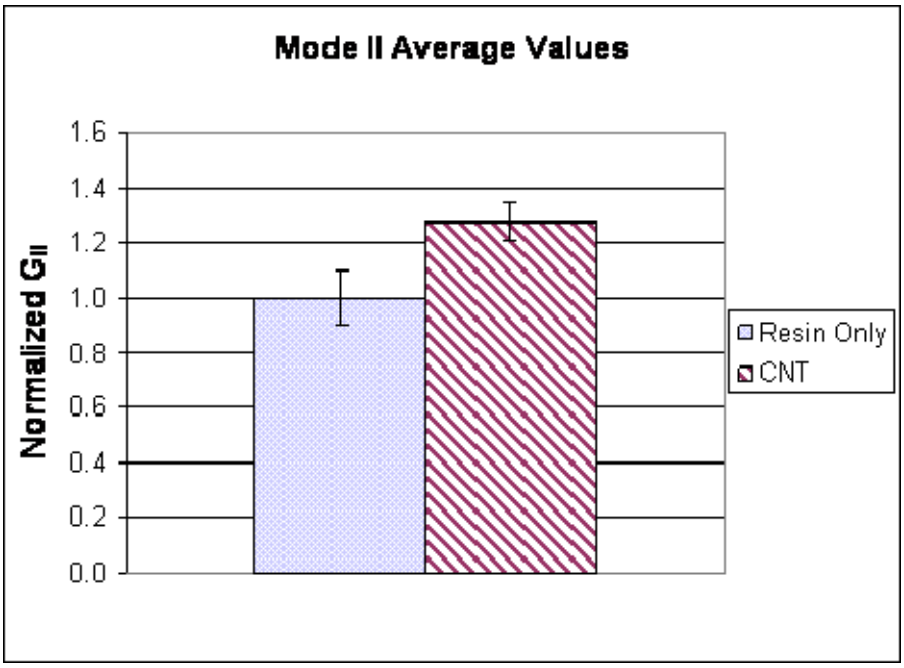

Figure 19. Mode II Normalized G_{II} Values

The Mode II critical energy release rate calculation was then repeated using a compliance approach. Compliance was determined from the linear region of the load versus displacement plot. Representative plots are shown in Figures 20 and 21. A linear regression was used to obtain the slope of the linear region. The point of crack propagation is marked with an *X*.

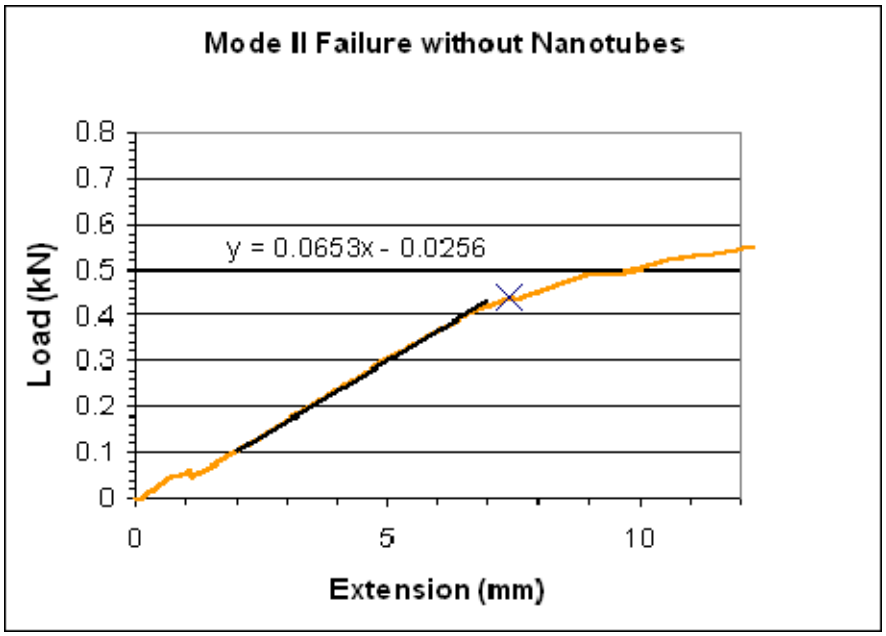

Figure 20. Representative load versus extension plot for Mode II (shear mode) testing of non-reinforced sample (The point of crack propagation is marked with an *X*.)

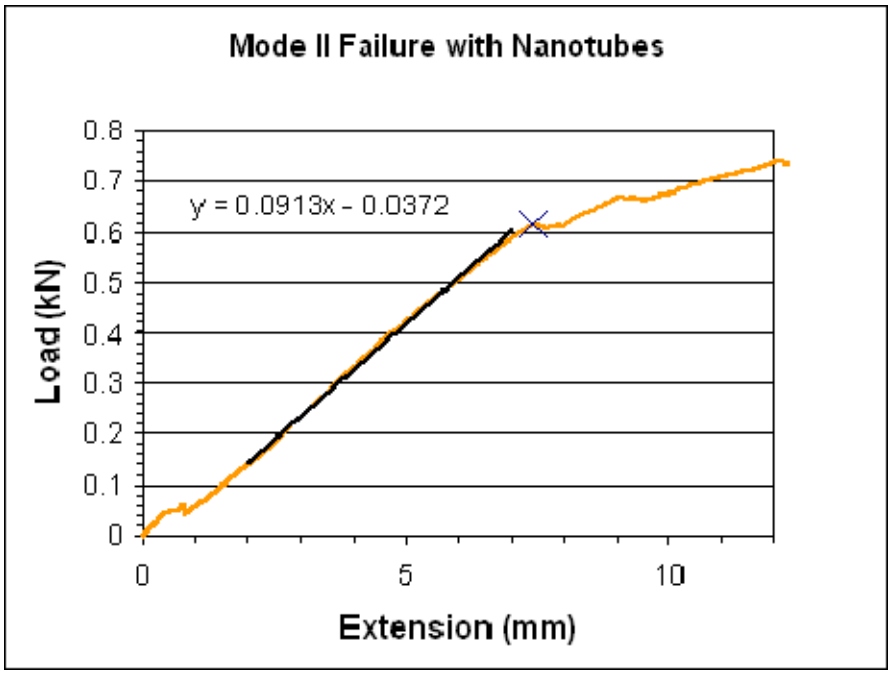

Figure 21. Representative load versus extension plot for Mode II testing of CNT reinforced sample

Repeating the calculation using a compliance approach showed a similar improvement in G_{II}. The average G_{II} value of CNT reinforced samples was 30.5% higher than that of the non-reinforced samples. Additionally, the lowest CNT reinforced value was higher than the highest non-reinforced value.

Since the method of locally reinforcing the samples with CNT significantly increased the value of Mode II critical energy release rate, testing was repeated using samples constructed via the VARTM technique since the VARTM technique is commonly employed by industry. Similar results were obtained when testing VARTM samples produced in Phase IV. Figure 22 displays the normalized average values of G_{II} for Phase IV specimens. Calculated via the compliance approach, the average G_{II} value of CNT reinforced samples was 31.6% higher than that of the non-reinforced samples. The implementation of local CNT reinforcement is promising due to these consistent results.

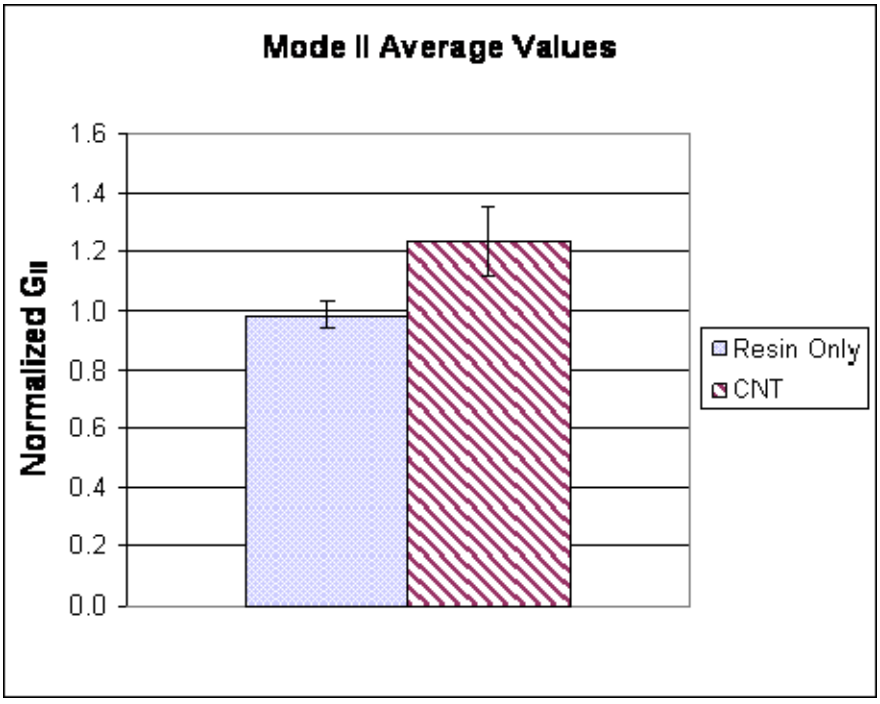

Figure 22. Mode II Normalized G_{II} Values for Phase IV samples

Qualitatively, the observed crack propagation was significantly different between the CNT reinforced and non-reinforced samples. In the non-reinforced samples, crack propagation began at the tip of the initial crack. However, this did not occur in the CNT reinforced samples. As the load increased, a crack began to occur away from the initial crack tip, perhaps in an area of lower CNT concentration, i.e., a weaker strength zone. Eventually, this new crack grew to meet the initial crack. This result was widely observed in the CNT reinforced samples. Figures 23 and 24 display images of the observed crack propagation. This phenomenon was observed in all phases of research. A representative image from the Digital Image Correlation System is shown in Figure 25. Shear strain is plotted at the onset of crack initiation since the shear stress is the cause of crack growth in Mode II.

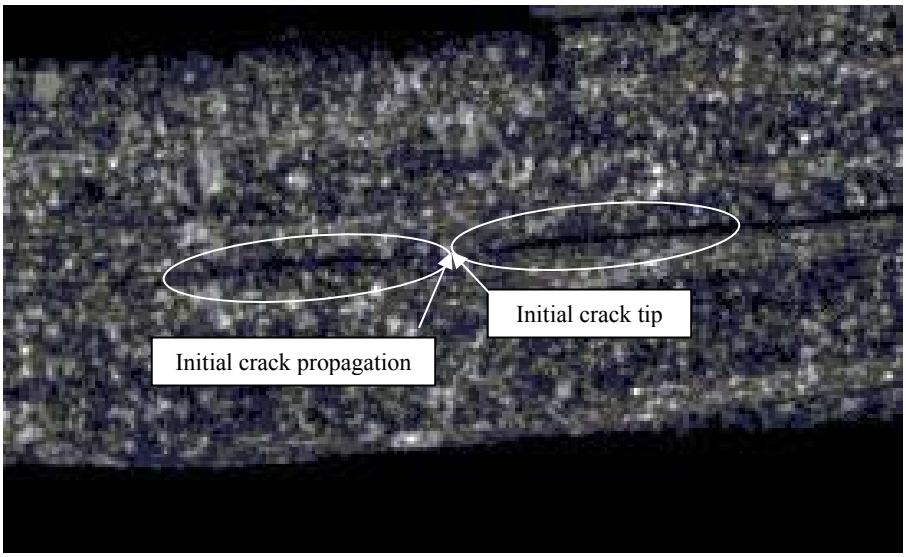

Figure 23. Initial crack propagation of resin only sample
(Crack propagated from the initial crack tip.)

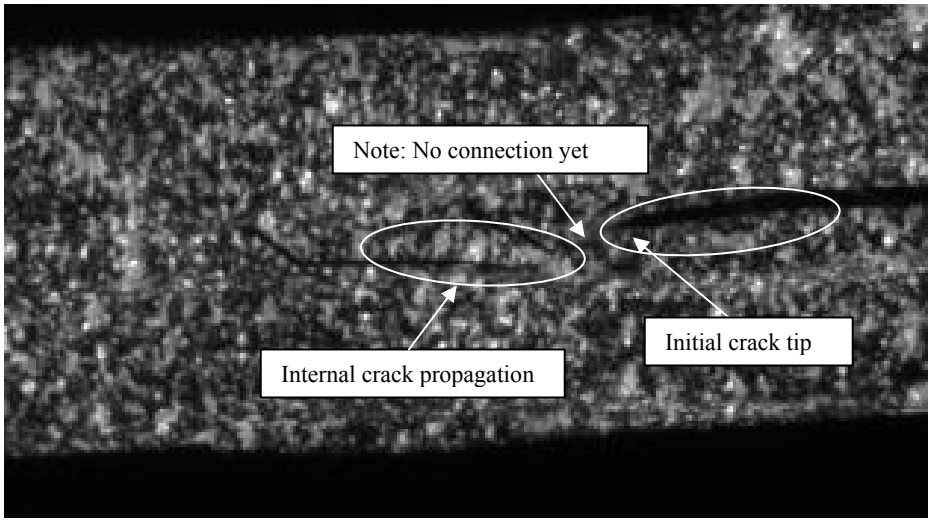

Figure 24. Initial crack propagation of CNT reinforced sample (The internal crack was nucleated away from the initial crack tip. Then the internal crack grew to meet the initial crack tip as the load increased.)

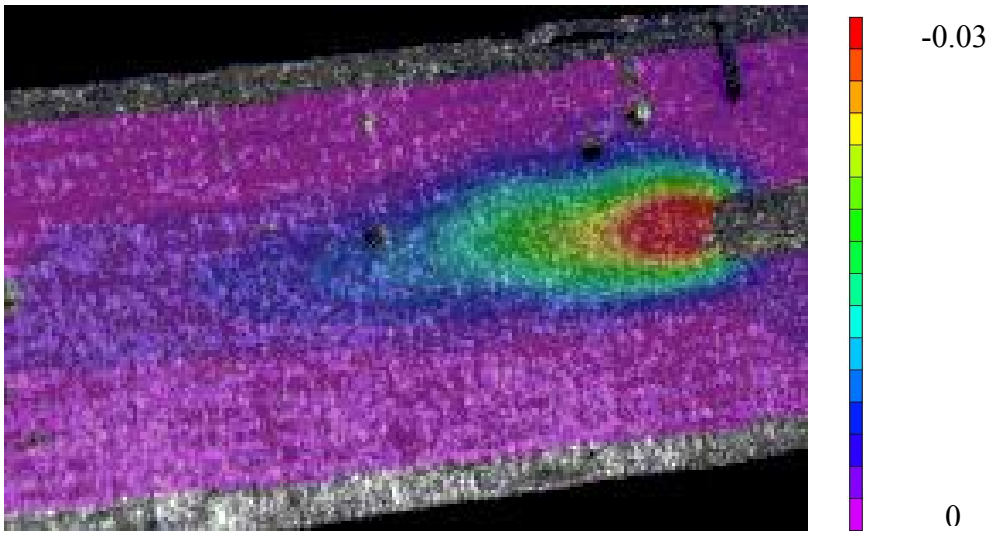

Figure 25. Plot of shear strain from Digital Image Correlation System for Mode II (i.e., shearing mode)

After testing, the samples were fully broken to inspect the cracked surface. Mode II crack propagation of the non-reinforced samples occurred at the interface of the initial crack site. In some areas, the joint interface bond was broken through the resin while in others the resin was pulled away from the fibers, as shown in Figure 26.

The CNT reinforced samples failed much differently. The CNT reinforced the resin, making it stronger. It is important to note that the CNT themselves did not fracture. The CNT bonded to the resin, blocking crack propagation. As a result, the crack propagated through the fibers, at times through a different layer than the initial crack layer. The critical energy release rate for CNT reinforced samples is higher because the crack propagated through the carbon fibers vice resin. Figure 27 shows an image of the cracked surface.

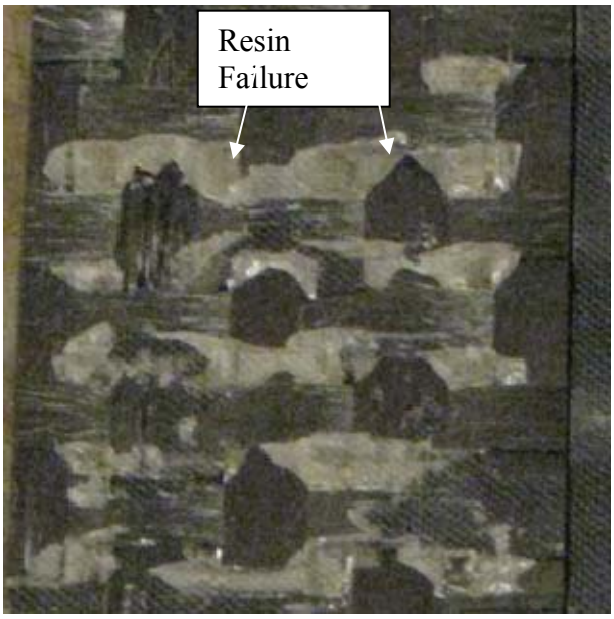

Figure 26. Mode II crack surface of non-reinforced sample (Note the crack propagated through resin. In some areas the resin failed and in others the resin pulled away from the fibers.)

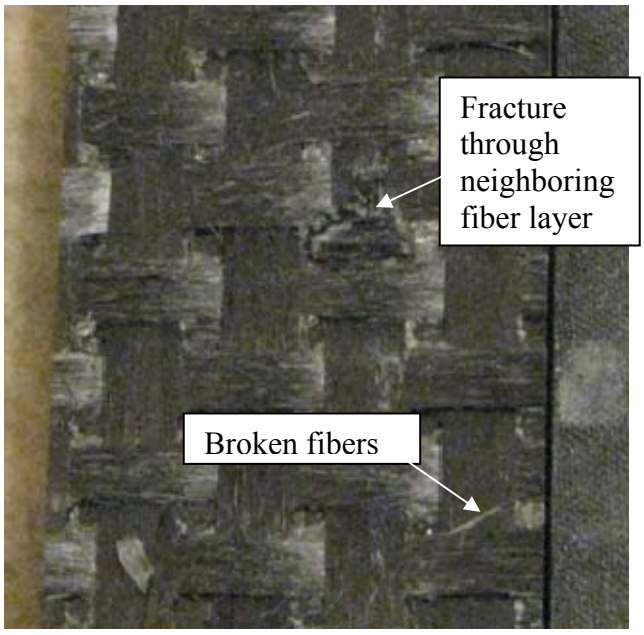

Figure 27. Mode II crack surface of CNT reinforced sample (Note the crack propagated through the fibers and through a neighboring fiber layer in one region.)

CNT reinforcement was significant during Mode II failure while not significant for Mode I. A possible explanation is given below for the application of CNT as an interface bond. When the CNT are applied, there are two surfaces to which they bond: cured resin and wet resin. The long polymer chains of the wet resin entangle the CNT. While the cured resin is not necessarily a smooth surface, the CNT do not have the opportunity to become entangled in the polymer chains because the resin is already cured. When the sample is cured, the CNT are entrapped in the polymer chains that were wet when the CNT were applied, as shown in Figure 28.

When a force is then applied normal to the bottom layer, the CNT have little effect, as in Mode I testing. However, when a force is applied along the surface, such as during Mode II testing, there is a mechanical interlocking between CNT and polymers, which makes the bond not easily broken. Then, the crack propagates through the fibers vice through the resin. As a result, the critical energy release rate is higher due to CNT reinforcement.

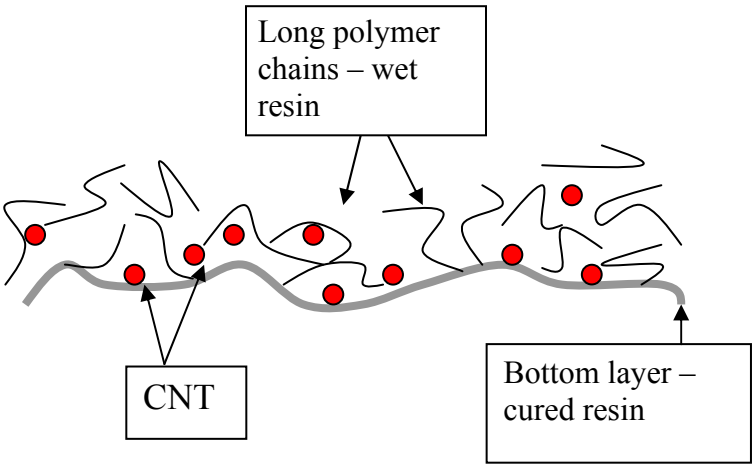

Figure 28. Schematic of secondary bond with CNT

C. MIXED MODE I/MODE II

Mixed Mode I/Mode II testing was conducted with the intention of determining a "best fit" formula for Mixed Mode I/Mode II calculations. However, when conducting the testing, technical problems arose. To conduct the test, piano hinges must be affixed to the samples to both apply load and secure the samples in the test apparatus. During the course of the test, the epoxy used to affix the piano hinges failed. Therefore, testing could not be completed. Crack propagation did occur in two non-reinforced samples, but results were inconclusive. Figure 29 displays Mode I, Mode II, and Mixed Mode I/Mode II data for non-reinforced samples. No CNT reinforced sample data was achieved for Mixed Mode I/Mode II testing.

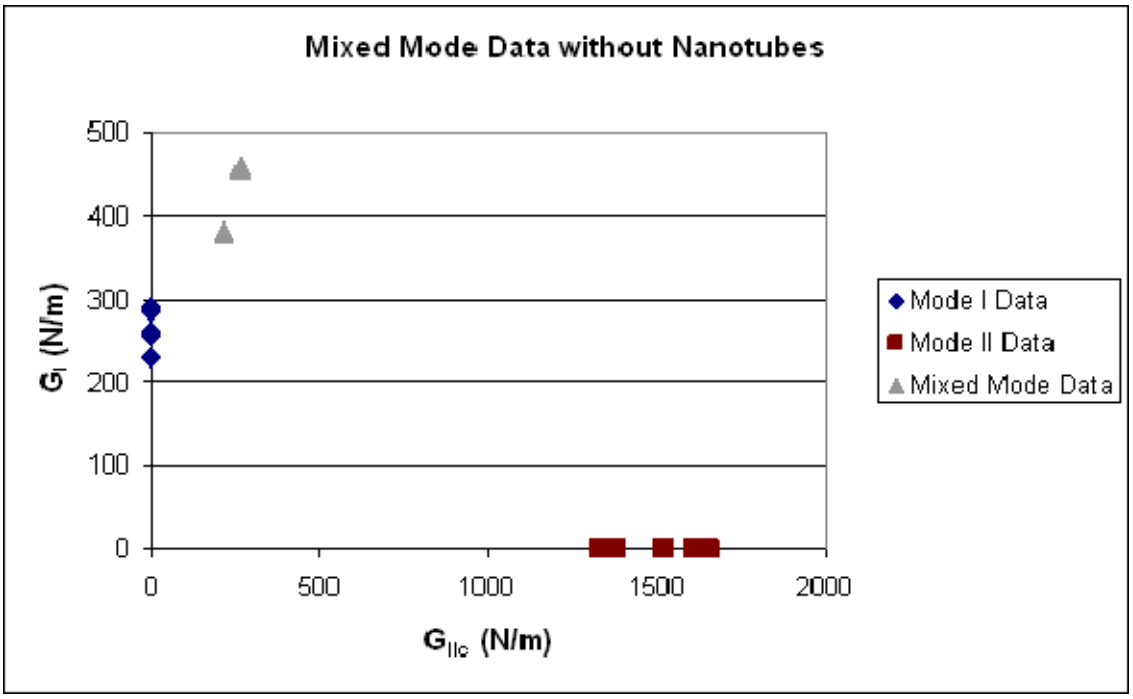

Figure 29. Plot of Mixed Mode I/Mode II data

D. SEAWATER ABSORPTION EFFECTS

Phase III samples were used to determine the effects of seawater absorption on Mode II critical energy release rate. Weight of each sample was tracked periodically during soaking, as shown in Figure 30. The samples were deemed saturated when no significant weight change occurred. In this case, the samples were tested after 91 days of soak. Samples were removed from the seawater, patted dry, and tested. It should be noted that the CNT reinforced samples absorbed slightly less seawater. During the hand lay-up process, a small amount of CNT migrates from the interface layer to neighboring layers. The resin near the CNT does not absorb as much seawater, resulting in a smaller percentage weight change. However, results of the testing were not significantly affected by the small difference in percentage weight change.

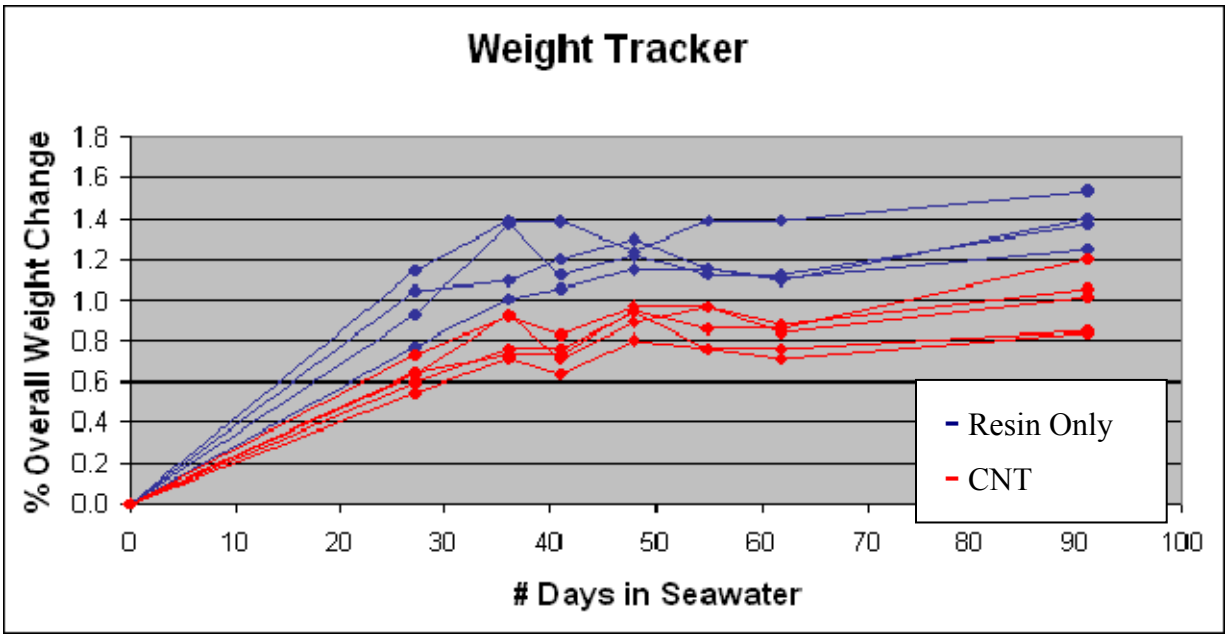

Figure 30. Seawater absorption weight tracker for Phase III samples

The results of moisture effects testing were similar to Mode II testing with no seawater absorption. CNT reinforcement resulted in a 35.6% increase in G_{II} as shown in Figure 31. Again, Figure 31 displays average, normalized values. Standard deviation is also shown. Furthermore, the non-normalized values were similar to values for dry samples. It can therefore be concluded that soaking the carbon fiber composite samples in seawater did not affect Mode II fracture toughness. G_{II} values for each sample are included in Appendix C. Soaking the samples in seawater also did not affect the impact of localized CNT reinforcement.

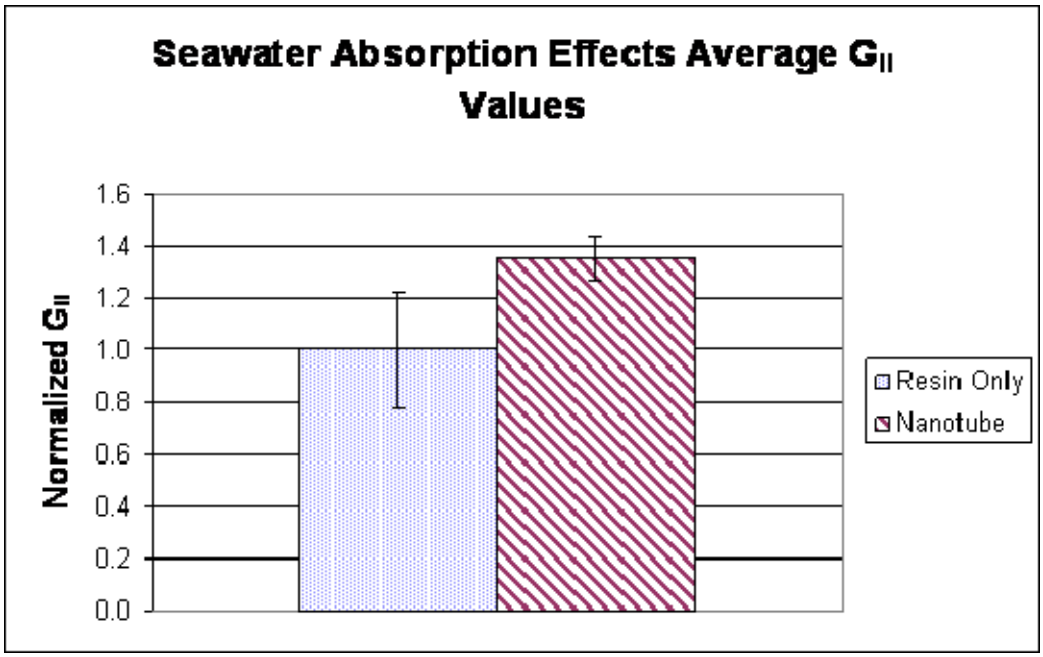

Figure 31. Mode II Normalized G_{II} Values for Phase III seawater soaked samples

To further study the effects of seawater absorption, samples constructed via the VARTM technique in Phase IV were soaked and tested. Again, the samples were deemed saturated when no significant weight change occurred. In this case, the samples were tested after 64 days of soak. Samples were removed from the seawater, patted dry, and Mode II testing was completed.

The percentage weight change for Phase IV samples was slightly lower than that of Phase III samples. The difference is due to the relative concentrations of resin and carbon fiber fabric. Phase III samples were produced via the hand lay-up technique, and therefore contain relatively more resin than Phase IV samples, which were produced via the VARTM method. Since seawater is absorbed by the resin, the Phase III samples had a higher percentage weight change. Since Phase IV samples were constructed via the VARTM technique, the non-reinforced and CNT reinforced samples absorbed nearly the same amount of seawater. There was no difference in percentage weight change between resin only and CNT samples, as in the Phase III samples.

Phase IV seawater soaked samples yielded very different results from Phase III seawater soaked samples. During Mode II testing, the majority of samples failed in bending, as shown in Figures 32 and 33. The seawater absorption resulted in an overall stiffness reduction of the composite material, causing the samples to bend. The crack did propagate after bending failure initiated. However, the bending failure resulted in a shift of the neutral axis, meaning the initial crack was no longer on the neutral axis. When the three point bending test is conducted, the initial crack must lie on the neutral axis to determine pure Mode II critical energy release rate. As a result, Mixed Mode I/Mode II crack propagation occurred, and the calculation of Mode II critical energy release rate is no longer valid [15]. It is necessary to extract Mode I and Mode II energy release rates from the test results. However, the calculation requires the correct data of bending failure just before the interface crack propagation. In order to avoid the bending failure, it is recommended to have thicker specimens for future testing. Thick specimens will allow the interface crack to propagate before failure caused by bending stress.

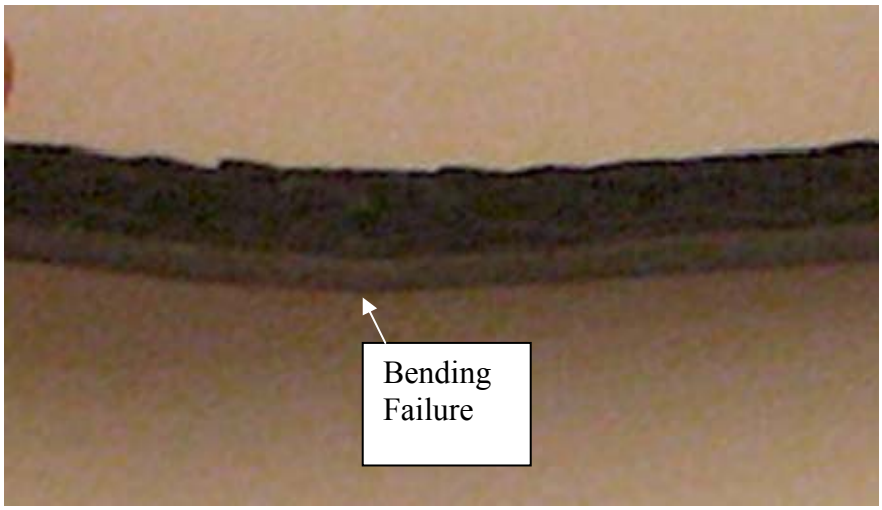

Figure 32. Bending failure of Phase IV seawater soaked sample (side view)

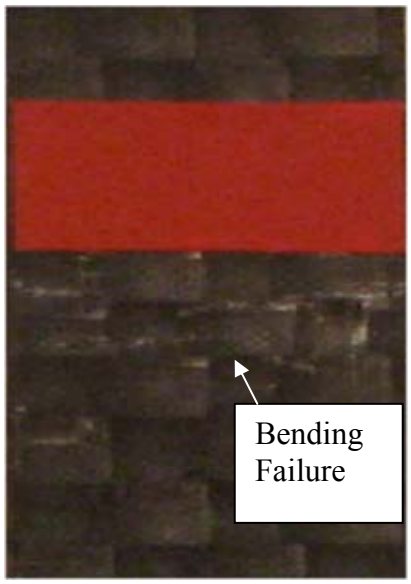

Figure 33. Bending failure of Phase IV seawater soaked sample (top view)

E. CNT OPTIMIZATION

The main purpose of Phase V samples was to optimize the concentration of CNT. To achieve this goal, three concentrations of CNT were used: 5 g/m^2, 7.5 g/m^2, and 10 g/m^2. As with all sample sets, non-reinforced samples were constructed and tested as a reference point. Mode II testing was completed since prior phases determined CNT reinforcement significantly affects Mode II fracture toughness. The results of Mode II testing are shown in Figure 34 along with standard deviation. As shown, 7.5 g/m^2 of CNT is the optimal concentration, which is consistent with the previous study on CNT compression strength improvements [9]. Again, the lowest value of G_{II} for samples reinforced with 7.5 g/m^2 CNT is higher than the highest value of non-reinforced samples. The G_{II} value for each sample is included in Appendix D.

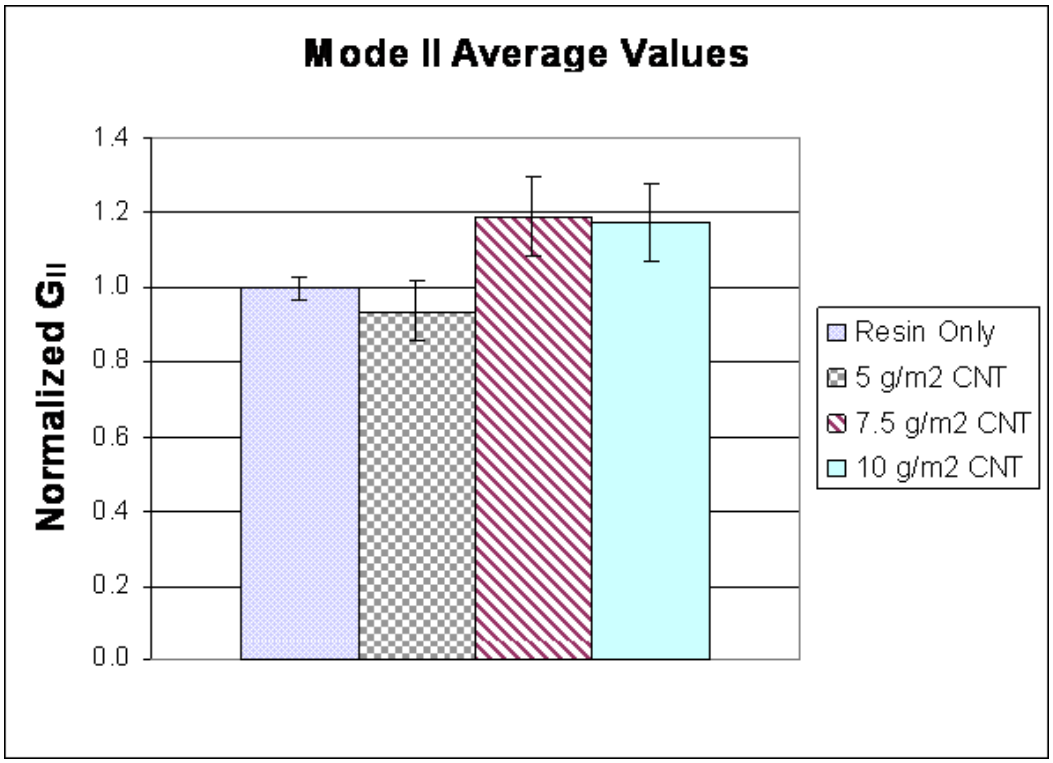

Figure 34. Mode II Normalized G_{II} Values for CNT Optimization samples

The secondary purpose of Phase V was to determine the effect of "banding" CNT. "Banding" refers to only reinforcing a part of the interface area on the sample. All other sample sets involved using CNT to reinforce the entire secondary bond between the top and bottom plates. Phase V samples were only reinforced in the area extending 6 cm from the initial crack tip. "Banding" CNT may be applicable to repair of carbon fiber composite components when only a localized area requires reinforcement. The Mode II critical energy release rate, as calculated via the compliance method, resulted in 18.8% increase due to CNT reinforcement with 7.5 g/m^2 CNT concentration. The drop from roughly 30% found in previous sample sets is due to "banding" the CNT vice reinforcing the entire secondary bond.

THIS PAGE INTENTIONALLY LEFT BLANK

VI. CONCLUSIONS AND RECOMMENDATIONS

In conclusion, critical energy release rate, G, and crack propagation characteristics of a pre-existing crack were studied in carbon fiber composite samples. Five phases of research were completed, each consisting of non-reinforced samples and samples reinforced with carbon nanotubes. Mode I (i.e., opening mode), Mode II (i.e., shearing mode) and Mixed Mode I/Mode II crack propagation were studied. Mode I testing determined no significant increase in G_I due to CNT reinforcement. Also, no differences in crack propagation were observed. However, Mode II testing determined a significant increase in G_{II} due to CNT reinforcement. Additionally, two qualitative differences were noted during Mode II testing as stated below:

1. CNT reinforced samples displayed crack nucleation and growth away from the initially existing crack tip. As load increased, these cracks propagated to meet the existing initial crack. For non-reinforced samples, crack propagation occurred from the existing initial crack tip.

2. Crack propagation occurred across the fibers in CNT reinforced samples. Conversely, crack propagation in non-reinforced samples occurred due to resin failure.

Additional research was conducted to determine the effects of seawater absorption and optimize the concentration of CNT. Seawater absorption was found to have no effect on Mode II fracture toughness. The optimal concentration of CNT was found to be 7.5 g/m^2. Finally, the VARTM technique was implemented to ensure local CNT reinforcement is feasible using current manufacturing practices. It was determined that the dispersed CNT remain in place while the carbon fiber layers are infused with resin.

Further research is necessary to determine the impact of CNT reinforcement in Mixed Mode I-Mode II failure. In actual structures, the stress will rarely be purely Mode I or Mode II. Further research is also needed to determine feasible manufacturing practices for local CNT dispersion.

THIS PAGE INTENTIONALLY LEFT BLANK

APPENDIX A: MODE I DATA

PHASE III

Resin Only

Sample	G_{IC} (N/m)
1	2.84E+02
2	2.61E+02
3	2.56E+02
4	2.29E+02
5	2.90E+02

CNT Reinforced

Sample	G_{IC} (N/m)
1	2.76E+02
2	2.83E+02
3	3.17E+02

THIS PAGE INTENTIONALLY LEFT BLANK

APPENDIX B: MODE II DATA

PHASE III

Resin Only

Sample	G_{IIc} (N/m)
1	1.33E+03
2	1.61E+03
3	1.52E+03
4	1.38E+03
5	1.66E+03
6	1.62E+03

CNT Reinforced

Sample	G_{IIc} (N/m)
1	1.91E+03
2	2.02E+03
3	1.94E+03
4	1.80E+03
5	2.07E+03
6	2.17E+03

PHASE IV

Resin Only

Sample	G_{IIc} (N/m)
1	1.50E+03
2	1.38E+03
3	1.48E+03
4	1.51E+03
5	1.49E+03

CNT Reinforced

Sample	G_{IIc} (N/m)
1	2.00E+03
2	1.78E+03
3	1.90E+03
4	2.08E+03

THIS PAGE INTENTIONALLY LEFT BLANK

APPENDIX C: SEAWATER ABSORPTION EFFECTS DATA

PHASE III

Resin Only

Sample	G_{IIc} (N/m)
1	1.30E+03
2	1.90E+03
3	1.28E+03
4	1.37E+03

CNT Reinforced

Sample	G_{IIc} (N/m)
1	1.88E+03
2	2.06E+03
3	1.87E+03
4	2.12E+03

THIS PAGE INTENTIONALLY LEFT BLANK

APPENDIX D: PHASE V DATA

PHASE V

Resin Only

Sample	G_{IIc} (N/m)
1	1.55E+03
2	1.54E+03
3	1.57E+03
4	1.66E+03
5	1.57E+03

5 g/m^{2}CNT Reinforced

Sample	G_{IIc} (N/m)
1	1.64E+03
2	1.47E+03
3	1.57E+03
4	1.33E+03
5	1.38E+03

7.5 g/m^{2}CNT Reinforced

Sample	G_{IIc} (N/m)
1	1.89E+03
2	1.85E+03
3	2.12E+03
4	1.65E+03
5	1.87E+03

10 g/m^{2}CNT Reinforced

Sample	G_{IIc} (N/m)
1	2.04E+03
2	1.94E+03
3	1.76E+03
4	1.66E+03

THIS PAGE INTENTIONALLY LEFT BLANK

LIST OF REFERENCES

[1] A. P. Mouritz, E. Gellert, P. Burchill, K. Challis, "Review of Advanced Composite Structures for Naval Ships and Submarines," *Composite Structures*, v. 53, pp. 21-41, July 2001.

[2] B. Jones, "VT Durability and U of Maine Fracture Program Seminar: Introduction to Navy Joints Design," NSWC Carderock Division, February-March 2006.

[3] V. K. Ganesh, T. S. Choo, "Modulus Graded Composite Adherends for Single-Lap Bonded Joints," *Journal of Composite Materials*, v 36, pp. 1757-1767, 2002.

[4] William D. Callister, Jr, *Materials Science and Engineering: An Introduction*, ed. 7, John Wiley and Sons, Inc, New York, 2007, pp. 433.

[5] E.T. Thostenson, Z. Ren, and T. Chou, "Advances in the Science and Technology of Carbon Nanotubes and Their Composites: A Review," *Composites Science and Technology*, v. 61, pp. 1899-1912, June 2001.

[6] M. Wong, M. Paramsothy, X.J. Xu, Y. Ren, S. Li, and K. Liao, "Physical Interactions at Carbon Nanotube-Polymer Interface," *Polymer*, v. 44, issue 25, pp. 7757-7764, December 2003.

[7] M. Cadek, J.N. Coleman, K.P. Ran, V. Nicolose, G. Bister, A. Fonseca, J.B. Nagy, K. Szostzk, F. Beguin, and W.J. Blau, "Reinforcement of Polymers with Carbon Nanotubes: The role of nanotube surface area," *Nano Letters*, v. 4, no. 2, pp. 353-356, February 2004.

[8] L. S. Schadler, S.C. Giannaris, P.M. Ajayan, "Load Transfer in Carbon Nanotube Epoxy Composites," *Applied Physics Letters*, v. 73, no. 26, pp. 3842-3844, December 1998.

[9] Y. W. Kwon, R. Slaff, S. Bartlett, and T. Greene, "Enhancement of Composite Scarf Joint Interface Strength through Carbon Nanotube Reinforcement," *Journal of Materials Science*, doi: 10.1007/s10853-008-2689-8, 2008

[10] ASTM Standard D 5528-01, "Mode I Interlaminar Fracture Toughness of Unidirectional Fiber-Reinforced Polymer Matrix Composites," March 2002.

[11] J. R. Reeder, "An Evaluation of Mixed-Mode Delamination Failure Criteria," NASA Technical Memorandum 104210, February 1992.

[12] M. Todo, T. Nakamura, K. Takahashi, "Effects of Moisture Absorption on the Dynamic Interlaminar Fracture Toughness of Carbon/Epoxy Composites," *Journal of Composite Materials*, v 34, pp. 630-648, 2000.

[13] ASTM Standard D 6671/D 6671M-06, "Standard Test Method for Mixed Mode I-Mode II Interlaminar Fracture Toughness of Unidirectional Fiber Reinforced Polymer Matrix Composites," March 2006.

[14] ASTM Standard D 1141-98, "Standard Practice for the Preparation of Substitute Ocean Water," August 2008.

[15] J. G. Williams, "On the Calculation of Energy Release Rates for Cracked Laminates," *International Journal of Fracture*, v 36, pp. 101-119, 1988.

INITIAL DISTRIBUTION LIST

1. Defense Technical Information Center
   Ft. Belvoir, Virginia

2. Dudley Knox Library
   Naval Postgraduate School
   Monterey, California

3. Graduate School of Engineering and Applied Sciences
   Naval Postgraduate School
   Monterey, California

4. Erik A. Rasmussen
   Naval Surface Warfare Center Carderock Division
   West Bethesda, Maryland

5. Scott W. Bartlett
   Naval Surface Warfare Center Carderock Division
   West Bethesda, Maryland

6. Douglas C. Loup
   Naval Surface Warfare Center Carderock Division
   West Bethesda, Maryland

7. Chris A. Hicks
   Northrop Grumman Ship Systems
   Gulfport, Mississippi

8. Joe Johnson
   Integrated Composites Inc.
   Marina, California

9. John Dickie
   Integrated Composites Inc.
   Marina, California

10. John McWaid
    Integrated Composites Inc.
    Marina, California

11. Professor Young W. Kwon
    Naval Postgraduate School
    Monterey, California

12. Professor and Chairman Knox T. Millsaps
Naval Postgraduate School
Monterey, California

13. Susan D. Faulkner
Naval Postgraduate School
Monterey, California